Copyright © Smart/Micro Grid Research Center, 2020
Electrical Power and Energy Systems 118 (2020) 105735

Contents lists available at ScienceDirect

Electrical Power and Energy Systems

journal homepage: www.elsevier.com/locate/ijepes

Stochastic optimal robust design of a new multi-stage under-frequency load shedding system considering renewable energy sources

Ali Rafinia, Jamal Moshtagh*, Navid Rezaei

Department of Electrical Engineering, University of Kurdistan, Sanandaj, Iran

ARTICLE INFO

Keywords:
Under-frequency load shedding
Contingency
Load fluctuations
Wind power
Solar power

ABSTRACT

The ever-increasing penetration of Renewable Energy Sources (RESs) into the power system has faced system operators with higher risks subject to a growing level of the associated uncertainties. To preserve the system frequency security, an under-frequency load shedding (UFLS) scheme can usually be utilized as a final remedial action, which is aimed at removing the excessive load. UFLS can be managed in a multi-stage portfolio based on the priority and sensitivity of the loads under control to cope optimally with the occurring power imbalances. Design of an optimal, robust UFLS scheme is a vital procedure. To that end, the present paper proposes a new UFLS protective system which is conducted to shed the minimum optimal load after precise detection of the frequency excursions. The problem is transferred into a Mixed-Integer Linear Programming (MILP) based optimization framework, and it is to be solved in several stochastic scenarios for setting the UFLS system parameters. The analysis of the UFLS setting results, which are extracted through implementation of the model on the IEEE 39-bus test system, demonstrates the effectiveness of the proposed MILP-based methodology in dealing with the severe uncertainties resulting from RES output variations and load fluctuations.

1. Introduction

1.1. Motivations

Nowadays, owing to power system deregulation and environmental motivations, operators' tendency to integrate sustainable utilization of Renewable Energy Sources (RESs) has been promoted greatly [1,2]. Recently, RESs have been widely developed, and has increased the efficiency of the system. Alongside these developments, the power system operator's tendency to use these energies has increased, and has led to RES penetration in power systems worldwide for economic-environmental reasons. Moreover, the competitive price of an RES compared to those of other energy sources such as fossil fuels has increased the benefits of using these sources [3].

The intermittent, uncertain output of these sources can have undesirable effects on security, power quality, and the stability of the power system [4]. By integrating these sources to the system, the power system operator reduces the generation capacity of the main generators, and, consequently, decreases system inertia [5]. Reduction of the inertia of the system and the oscillatory behavior of the RES puts the system frequency at risk [6].

For economic reasons, a power system is operated near its stability boundaries, and safe operation of the system depends on its voltage and frequency control within the permissible range [7]. All modern power systems are exposed to unusual operation conditions such as common network faults, loss of the power generation, sudden increases in load, constant variations in the RES output, and other disturbances that lead to a reduction of system capacity. In such conditions, the balance between the existing load and the remaining generation must be restored so that the frequency drop does not cause system blackout. If the governor is not fast enough, or the spinning reserve is insufficient to restore the system frequency, the automated UFLS system can be used as the latest system recovery to prevent collapse [8,9].

Various automated UFLS systems are capable of predicting and controlling load shedding in the under-frequency conditions at several stages with minimal time delays. In several power systems, Rate Of Change Of Frequency (ROCOF) is used as an additional factor for load shedding, and the frequency set-points are selected based on extraordinary emergencies that are more probable for a specific power system [10]. The model to be considered for designing an automated UFLS system should include the different dynamics of the system generators, load parameters, and under-frequency relay setting indices [11]. Hence, the design of an optimal UFLS scheme, which is capable of robustly facing frequency excursions stemming from uncertain resources, can be a vital procedure in preservation of system sustainability.

* Corresponding author.
E-mail address: j.moshtagh@uok.ac.ir (J. Moshtagh).

https://doi.org/10.1016/j.ijepes.2019.105735
Received 22 July 2019; Received in revised form 15 October 2019; Accepted 22 November 2019

Nomenclature

Indices

i	generation units
sc	scenario
s	stage of load shedding
c	under-frequency threshold of generators specified by manufacturer
n	time step of discrete simulation

Parameters

f_0	nominal frequency
H_i	inertia time constant of unit i
R_i	governor droop of unit i
S_i	power base of unit i
S	power base of system
f_c	threshold of generators under-frequency specified by manufacturer
π^{sc}	probability of scenario sc

Continuous variables

ΔGI^{sc}	loss of generation due to scenario sc
Δf_n^{sc}	frequency deviation from nominal value due to scenario sc at time step n
ΔFR_n^{sc}	primary frequency regulation due to scenario sc at time step n
f_s	set-point of frequency at stage of load shedding s
LSH_s	load shedding amount at stage of load shedding s
Δt_s	time delay of under-frequency relay at stage of load shedding s
$\Delta t_{s,n}^{sc}$	time delay of under-frequency relay below set-point f_s due to scenario sc at time step n
$\Delta t_{c,n}^{sc}$	time delay of under-frequency relay below the threshold f_c due to scenario sc at time Step n
ΔP_w^{sc}	wind power variations due to scenario sc
ΔP_{pv}^{sc}	solar power variations due to scenario sc
ΔP_{lf}^{sc}	load fluctuations duo to scenario sc

Binary variables

$V_{s,n}^{sc}$	one, if $\Delta f_n^{sc} < f_s$due to scenario sc at time step n, otherwise zero.
$U_{s,n}^{sc}$	one, if $\Delta t_{s,n}^{sc} > \Delta t_s$ and $f < f_s$ due to scenario sc at time step n, otherwise zero.
$W_{c,n}^{sc}$	one, if $f < f_c$ due to scenario sc at time step n, otherwise zero.

Abbreviations

UFLS	under-frequency load shedding
ELNS	expected load not supplied
MCS	Monte-Carlo simulation
MILP	mixed-integer linear programming
PDF	probability density function
PV	photovoltaic
RWM	roulette wheel mechanism

1.2. Literature review

Different types of research have addressed the UFLS setting problem. The primary purpose of the UFLS strategies is minimizing the total amount of the load shedding and increase the reliability, security, and sustainability of the system and consumer social welfare. In [12], a new systematic approach is proposed for the setting of the under-frequency relays for a replacement for many trial and error based methods. Here, a new formulation for several outages of generation units and considering characteristics such as inertial and damping constants are presented. The objective function is minimizing the load shedding amount for a set of contingencies of the generation units. By using the optimization method of mixed-integer linear programming (MILP), the under-frequency relay can be useful in preventing the power system collapse. Ketabi et al. [13] have proposed a UFLS-based method for minimum system prediction frequency, in which the system frequency is sampled after contingency. Then, the samples are used to predict the minimum system frequency based on the Particle Swarm Optimization (PSO) algorithm. In this paper, with the least error, a precise estimation of the system parameters has been made. The UFLS scheme is presented in [14] that reduces the amount of load shedding by estimating the power deficiency with continuous monitoring of the second derivative of the frequency of the inertial center. Then, by determining an equivalent inertial constant for estimating the system power loss, the best load combination is determined by the Particle Swarm Optimization (PSO) algorithm, and the minimum and maximum frequencies are minimized. Zhenglong et al. [15], an optimal process for under-frequency relays setting in the regional power system, is presented. Here, an improved multi-generator frequency response (IMFR) model is designed for accurate measurement of the system frequency after an imbalance between generation and consumption. The proposed IMFR include spinning reserve, various governors, and static load model and also selects the contingencies for designing the UFLS. In [16], the probabilistic UFLS scheme is formulated as a mixed-

Table 1
Taxonomy table of the UFLS problem.

Reference	Uncertainty resource				Solving strategy			Optimized linearization of the model		Relay parameters		
	Wind	Solar	Generation deficiency	Load fluctuation	Heuristic	AI	MILP			f_s	LSH_s	Δt_s
[12]			*				*			*	*	*
[13]			*		*					*	*	
[14]			*		*					*	*	
[15]			*				*	*		*	*	*
[16]			*				*	*		*	*	*
[17]			*							*	*	*
[18]	*		*		*					*	*	
[19]			*			*				*	*	*
[20]			*		*	*				*	*	*
[21]	*		*					*		*	*	
This paper	*	*	*	*			*	*		*	*	*

integer linear program (MILP) problem to minimize the total amount of load shedding. The uncertainties of the proposed scheme using the point estimate method are modeled, and the results are compared with the Monte-Carlo simulation (MCS) method. In this paper, the BONMIN solver is used for the proposed UFLS. Amraee, Darebaghi, and Soroudi [17] using the MILP approach have proposed a method for the under-frequency load shedding, which by this method sheds the optimal value from the load. In this paper, the ROCOF relay is used to protect the anti-islanding of Distributed Generators (DGs) on the IEEE 39-bus. The MCS method is used for considering the uncertainties of system parameters. In this method, the results of load shedding are desirable. In [18], a hierarchical genetic algorithm is used to minimize the amount of load shedding. In this paper, the percentage of load permissible to be shed is determined to minimize frequency oscillation. The relay parameters, including the number of stages and time delay have been obtained for the under-frequency relay (81L). In [19], a UFLS scheme by implementing an artificial neural network (ANN) and transient stability analysis is presented. To provide the training data set, the transient stability analysis has been accomplished to minimize the load shedding amount with different operation scenarios. Moazzami et al. [20] utilized a fast load shedding method based on the ANN. In this paper, the amounts of active and reactive power to be shed are optimized using a priority list by PSO co-evolutionary algorithm and ANN method. All simulations are performed on the IEEE 118-bus, and ANN training data is based on contingency analysis on this system In [21], a remedial action scheme (RAS) for the fast load shedding is expanded considering wind generation. In the proposed RAS, the dynamics of wind farms are considered in the load shedding process, and an efficiency index is obtained according to the contribution of each generator to the dynamic performance of the system, and all formulas are written based on this index.

Table 1 provides a summarized comparison of the previous research on the under-frequency load shedding strategy and the present study. According to this table, in most of the existing works, there is no comprehensive discussion of the kinds of problem that the power system may be faced with. To fill this gap in this paper, uncertainty resources such as generation deficiency due to contingencies, variations in the RES output, and load fluctuations are considered for optimal setting of the under-frequency relay parameters for minimization of the amount of load shedding by the MILP formulation.

1.3. Contributions

In order to increase the efficiency of the UFLS scheme, this paper presents a new UFLS strategy in the IEEE 39-bus test system. In the setting of the under-frequency relay, the uncertainty involved in the RES and in load fluctuation has been included as well as that of contingency. Thanks to the Monte-Carlo Simulation (MCS) approach, three scenarios are generated using a process containing MCS, Roulette Wheel Mechanism (RWM), and the scenario reduction algorithm. Then, three parameters including the load shedding block, frequency threshold, and time delay of the under-frequency relay are optimally obtained using Mixed-Integer Linear Programming (MILP). Hence, the relay timer model, relay operating logic model, and relevant constraints are included. Therefore, the main contributions of the paper are highlighted below:

- Development of a time-discrete MILP with the CPLEX solver for precise setting of under-frequency relays
- Ensuring the UFLS scheme performance concerning the uncertainty resulting from generation deficiency, RES, and load fluctuations by providing an efficient optimization portfolio
- Efficient, detailed relay setting extraction involving the step-based frequency threshold, load to be shed, and time delay frequency considering the impact of RES uncertainties'.

This paper is organized as follows. The model description and problem formulation of the proposed UFLS are presented in Section 2. Section 3 shows the results of validation of the proposed method followed by its evaluation in the stochastic space, and analyzes the results. The results obtained by the proposed method are compared with those of other papers in Section 4. Finally, the paper is concluded in Section 5.

2. Model description and problem formulation

In this paper, an optimal MILP-based proposed stochastic program is proposed for implementation of the under-frequency setting, as follows. In the following sections, this model is explained in detail.

2.1. Generating and reducing the scenario

In this paper, the various uncertainties are considered using Monte

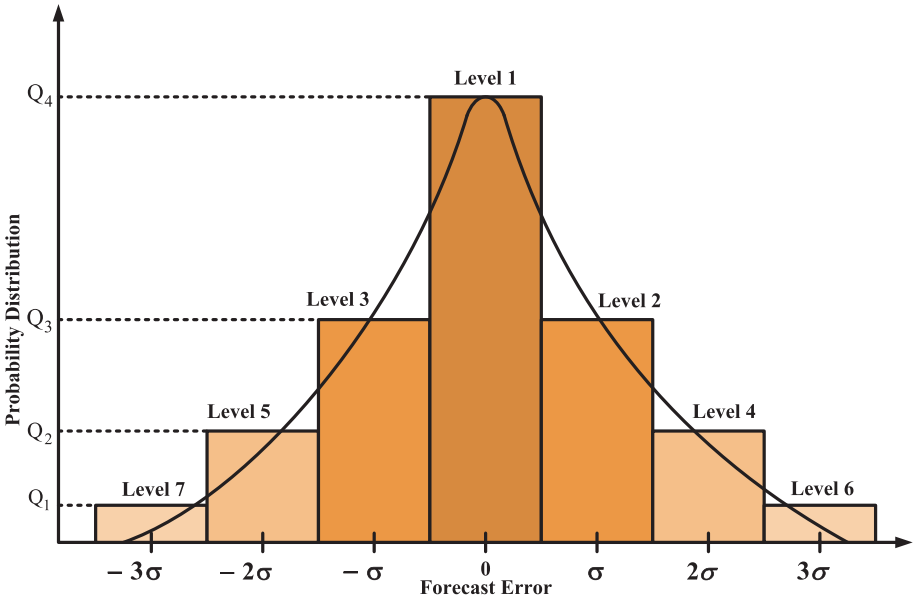

Fig. 1. Probability distribution function corresponding to the forecast error [24].

Carlo Simulation (MCS), and the scenarios with the highest probability (Q) of occurrence are selected. Hence, a Probabilistic Distribution Function (PDF) concerning the forecast error of generation deficiency, wind and solar generation, and load fluctuations should be generated with the appropriate accuracy. In the generation of the PDFs, previous statistical data on weather conditions, wind speed, and solar radiation in the system environment should be extracted. Fig. 1 shows the PDF of the forecast error associated with a particular uncertainty. This PDF can be discretized to several desirable intervals with various standard deviation errors (σ) resulting from zero error mean (μ) and different probability values attributed to each interval [22]. Then, according to the different levels of probability associated with the PDF, the Roulette Wheel Mechanism (RWM) is applied to generate the most probable scenarios. Therefore, according to Fig. 2, the probability corresponding to each level is normalized, so the sum of all the probability values is 1, and the normalized probability values are randomly divided between 0 and 1. Each random number is normalized to a forecast level in the roulette wheel, and is chosen as a scenario for that level. It is also necessary to use the scenario reduction algorithm to obtain the most probable scenarios [23].

The uncertainties affect all the specifications of the power system, such as electricity prices, network reliability, social welfare, and transmission line power. Therefore, the momentary variations in the uncertainties should be included, and an appropriate stochastic model should be used to illustrate these variations in the modeling of the uncertainties. Usually, the Weibull function is utilized to describe the distribution of wind power generation probability, which is a function of the wind speed in the network. With proper approximation, the normal distribution function (Gaussian) can be used instead of the Weibull function to model uncertainty [24]. Table 2 shows the mean and standard deviation values for wind and solar generation, load fluctuation, and generation deficiency. The histograms associated with the different uncertainties are presented in Fig. 3. To terminate the iterations required for generating scenarios, a stopping criteria based on mean (μ_f) and standard deviation (σ_f) values of forecasted parameters has been considered as can be expressed by $cv_f = \frac{\sigma_f}{\mu_f\sqrt{NS}}$. NS is total number of generated scenarios [24].

2.2. Proposed UFLS mathematical formulation

In this section, some basic concepts of the under-frequency relay and power system dynamics are presented, and the UFLS process is presented by the MILP formulation method for setting the under-frequency relays.

2.2.1. Power system dynamics

The imbalance between system generation and consumption causes changes in the turbine-generator speed, and so, the system frequency has large deviations. The swing equation of a generation unit is the relation between the active power and frequency response of the system, which is expressed mathematically in Eq. (1).

$$\frac{2H}{f_0}\frac{d\Delta f}{dt} = P_m - P_e = \Delta P \tag{1}$$

Here, $H = \sum_i \frac{H_i S_i}{S}$, $i = 1, \cdots, N_g$ is the inertia constant of the generator; $S = \sum_{i=1}^{N_g} S_i$ is the base power of the system; $P_m = \sum_{i=1}^{N_g} P_{mi}\frac{S_i}{S}$ is the mechanical input power; $P_e = \sum_{i=1}^{N_g} P_{ei}\frac{S_i}{S}$ is the electrical output power, Δf is the frequency deviation from the nominal value [25].

There are various types of electrical loads in the power system. The power consumption of motor loads, unlike resistive loads, is modified when frequency fluctuations occur. In these loads, the motor speed changes according to the input power frequency and decreases the power consumption by reducing the system frequency. The dependence of power consumption to the system frequency in motor loads is expressed by Eq. (2) [25]:

$$\Delta P_{motor} = D\Delta f \tag{2}$$

Here, ΔP_{motor} is the change of power consumption of motor loads, and D is the damping constant. The load sensitivity must be applied to the frequency variations in the swing equation. If the load damping in the under-frequency relay settings is not modeled, there is a probability of an excessive load shedding, and the resulting design will be very conservative [25].

The speed governor of the units in the interconnected power system is responsible for opposing changes in frequency by modifying its active power generation. Hence, for a frequency deviation, Δf, the governor would change the power output of the units. So, without a regulator, frequency variations would be unacceptable, and the relay would be improperly set. The governor's operation in the swing equation is Eq. (3) [25]:

$$\frac{2H}{f_0}\frac{d\Delta f}{dt} = \Delta P - \Delta P_{motor} + \Delta FR = P_m - P_e + \Delta FR - D\Delta f \tag{3}$$

Here, ΔFR is the primary frequency regulation.

2.2.2. Model of discrete time-frequency response

All in all, depending on parameters such as the inertial constant and the governor droop for multi-machine power system generators, each contingency for a generator has a unique frequency response. Accordingly, all the system generators swing simultaneously at a common frequency *f*. The frequency response of the system in the equivalent single-machine swing equation is written as Eq. (4):

$$\frac{d\Delta f(t)}{dt} = \frac{f_0}{2H}(\Delta FR(t) - \Delta GL(t) + LSH(t) - D\Delta f(t)) \tag{4}$$

Here, $\Delta GL(t)$ is a generation drop value at time t; $LSH(t)$ is the load shedding value at time t by the under-frequency relay action; $\Delta FR(t)$, the regulation of the primary frequency at time t with governor action and time constant T is obtained by Eq. (5):

$$\frac{d\Delta FR(t)}{dt} = \frac{1}{T}(-\Delta FR(t) - \frac{\Delta f(t)}{R}) \tag{5}$$

In Eq. (5), the equivalent governor droop is calculated as Eq. (6):

$$\frac{1}{R} = \sum_i \frac{S_i}{R_i S} \tag{6}$$

The system frequency response in Eqs. (4) and (5), is discretized into the time step Δt by defining $\Delta FR(n\Delta t) = \Delta FR_n$, $LSH(n\Delta t) = LSH_n$ and $\Delta f(n\Delta t) = \Delta f_n$, and through Euler's method, Eq. (4) is written in discrete form Eqs. (7) and (8):

$$\Delta f_n = \Delta f_{n-1} + ROCOF_{n-1}\Delta t \tag{7}$$

Here,

$$ROCOF_n = \frac{f_0}{2H}(\Delta FR_n - \Delta GL + LSH_n - D\Delta f_n) \tag{8}$$

Also, Eq. (5) in discrete form is given by Eq. (9):

$$\Delta FR_n = \Delta FR_{n-1} \times \left(1 - \frac{\Delta t}{T}\right) - \frac{\Delta t}{T} \times \frac{\Delta f_n}{R} \tag{9}$$

Given that there is no primary frequency deviation before a

Fig. 2. Roulette wheel mechanism for normalization of forecast error probability [24].

Table 2
Mean and standard deviation values of the various uncertainties.

PDF parameters	Wind generation (pu)	Solar generation (pu)	Load fluctuation (pu)	Generation deficiency (pu)
Mean μ	0.054	0.1	0.32	0.55
Standard Deviation σ	0.027	0.052	0.24	0.16

contingency, the initial conditions for equations Eqs. (7) and (9) are zero.

The under-frequency relays identify the under-frequency conditions in the power system by monitoring the bus frequency at each station and eliminating some of the load to prevent the system from becoming unstable. When the system frequency is less than a specific frequency, the relay timer turns on. Whenever a frequency deviation from the nominal value occurs and the time value of the relay timer exceeds Δt, the under-frequency relay sends the command to the circuit breaker to disconnect the LSH block; otherwise, the relay timer is reset. For an under-frequency relay with n_s load shedding stage, n_s sets of the three variables of the relay are determined under Eq. (10).

$$f_s,\ \Delta t_s,\ LSH_s,\ s = 1,\ \cdots, n_s \tag{10}$$

2.2.3. Use of binary variables in under-frequency relay setting

In this paper, the parameters setting of the under-frequency relay, in stochastic space are implemented as the MILP to minimize the appropriate objective function, subject to the following conditions: (1) In the frequency response of the power system versus time for the scenario *sc*, the under-frequency relay response must be considered; and (2) Time/frequency constraints determined by the manufacturer for generators should be respected.

The UFLS scheme with a certain number n_s of the load shedding stages in the scenario *sc*, for each load shedding stage *s*, the relays eliminated the LSH_s block in the time step *n*. In this time step, the frequency curve Δf_n^{sc} exceeds the frequency set-point f_0, for a length of the time higher than Δt_s. Here, the values of the relay settings $\{f_s, LSH_s, \Delta t_s\}$ are decision variables of the MILP. Also, the decision variable of the frequency deviation, Δf_n^{sc}, is obtained for the various scenarios *sc* at the time step *n* by the MILP. Hence, in the load shedding stage *s*, for each set-point of the frequency f_s, by the binary variable $V_{s,n}^{sc}$, a timer is defined by Eq. (11):

$$\frac{f_s - (f_0 + \Delta f_n^{sc})}{M_1} \le V_{s,n}^{sc} \le 1 + \frac{f_s - (f_0 + \Delta f_n^{sc})}{M_1} \tag{11}$$

It should be considered a condition Eq. (12) for the binary variable $V_{s,n}^{sc}$:

$$V_{s,n}^{sc} = \begin{cases} 0 & f_0 + \Delta f_n^{sc} > f_s \\ 1 & f_0 + \Delta f_n^{sc} < f_s \end{cases} \tag{12}$$

M_1 in Eq. (12) is a large positive value. The total time spent in the scenario *sc* is written below the frequency of the set-point f_s in the step of time *n* by the binary variable $V_{s,n}^{sc}$, by Eq. (13):

$$\Delta t_{s,n}^{sc} = \Delta t_{s,n-1}^{sc} + V_{s,n}^{sc}\Delta t \tag{13}$$

If the system frequency is higher than f_s, the timer is zero, which is shown in Eq. (14):

$$\Delta t_{s,n}^{sc} \le N \times V_{s,n}^{sc} \qquad \forall\ N \ge n \tag{14}$$

The relay operation logic expresses that if the frequency is smaller than f_s when $\Delta t_{s,n}^{sc} > \Delta t_s$, then the LSH_s block is shed. Here, the logic of the relay operation is modeled by Eq. (15) and the binary variable load shedding $U_{s,n}^{sc}$:

$$\frac{(\Delta t_{s,n}^{sc} - \Delta t_s)}{M_2} \le U_{s,n}^{sc} \le 1 + \frac{(\Delta t_{s,n}^{sc} - \Delta t_s)}{M_2} \tag{15}$$

Here, M_2 is a large positive number. Also, for the binary variable $U_{s,n}^{sc}$, the condition Eq. (16) is considered:

$$U_{s,n}^{sc} = \begin{cases} 0 & \Delta t_{s,n}^{sc} < \Delta t_s \\ 1 & \Delta t_{s,n}^{sc} > \Delta t_s \end{cases} \tag{16}$$

Also, Δt_s, is a variable, and according to Eq. (17), this variable must be higher than the minimum time needed to open the circuit breaker, Δt_{min}.

$$\Delta t_s \ge \Delta t_{min} \tag{17}$$

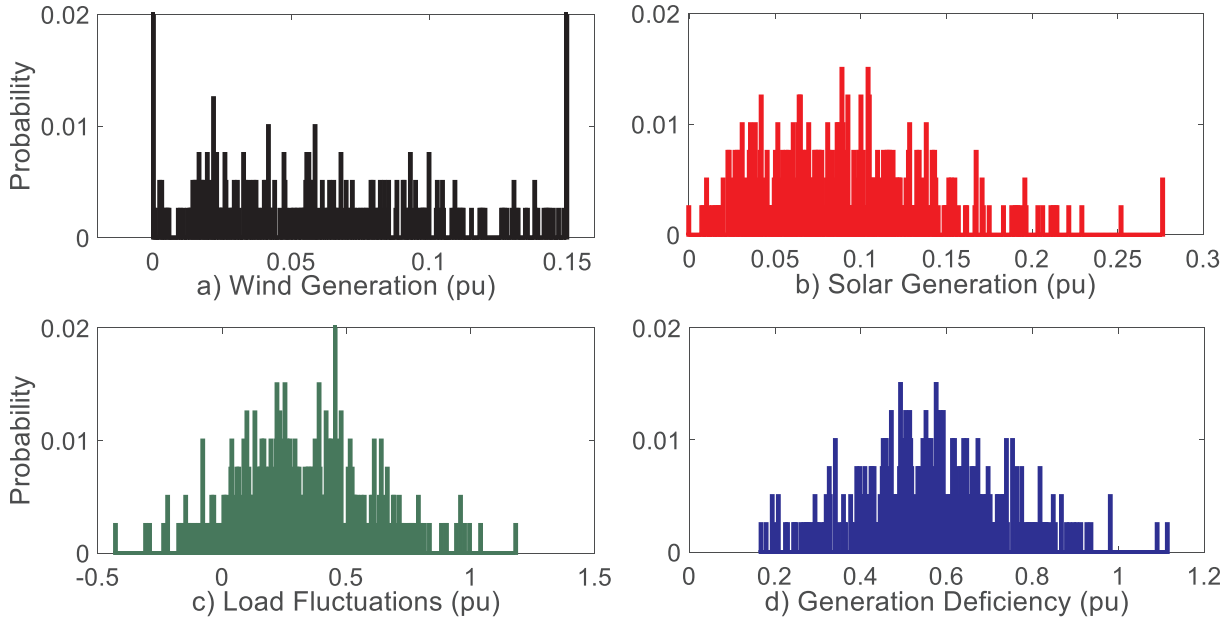

Fig. 3. Histograms of the various uncertainties.

It is assumed that some load that is shed in stage *s*, according to Eq. (18), are not restored at a later time:

$$U^{sc}_{s,n} \geq U^{sc}_{s,n-1} \tag{18}$$

Also, according to Eq. (19), the different stages of load shedding in the time step n for all stages s and scenario sc should not be simultaneously performed:

$$\sum_s U^{sc}_{s,n} - \sum_s U^{sc}_{s,n-1} \leq 1 \tag{19}$$

The next issue is that higher priority loads (such as critical loads including hospitals, military and security institutions) should not be shed at lower stages. This condition is expressed in Eq. (20):

$$U^{sc}_{s,n} \geq U^{sc}_{s+1,n} \tag{20}$$

Regarding Eqs. (7) and (9), the relation of discrete-time/frequency, for each scenario *sc*, is written as Eq. (21):

$$\Delta f^{sc}_n = \Delta f^{sc}_{n-1} + ROCOF^{sc}_{n-1}\Delta t \tag{21}$$

Here, the load shedding term $\sum_s U^{sc}_{s,n} \times LSH_s$ is added to Eq. (8) to consider the effect of the load shedding factor in the frequency response of the system. Therefore, the new equation is written as Eq. (22):

$$ROCOF^{sc}_n = \frac{f_0}{2H^{sc}}(\Delta FR^{sc}_n - \Delta GL^{sc} - D\Delta f^{sc}_n + \sum_s U^{sc}_{s,n} \times LSH_s) \tag{22}$$

In this equation, the primary frequency regulation is obtained as Eq. (23):

$$\Delta FR^{sc}_n = \Delta FR^{sc}_{n-1} \times \left(1 - \frac{\Delta t}{T}\right) - \frac{\Delta t}{T} \times \frac{\Delta f^{sc}_n}{R^{sc}} \tag{23}$$

In the load shedding factor $\sum_s U^{sc}_{s,n} \times LSH_s$, the discrete binary variable $U^{sc}_{s,n}$ is multiplied by the continuous load shedding value LSH_s, then the relationship $Z^{sc}_{s,n} = U^{sc}_{s,n} \times LSH_s$ must be written as Eqs. (24), (25) and (26):

$$0 \leq Z^{sc}_{s,n} \leq U^{sc}_{s,n} \tag{24}$$

$$0 \leq LSH_s - Z^{sc}_{s,n} \leq (1 - U^{sc}_{s,n}) \tag{25}$$

$$Z^{sc}_{s,n} = \begin{cases} LSH_s & U^{sc}_{s,n} = 1 \\ 0 & U^{sc}_{s,n} = 0 \end{cases} \tag{26}$$

The load shedding amount can be limited to a set of predefined blocks following Eq. (27):

$$LSH_s = LSHS_s \tag{27}$$

In this case, Eq. (22) should be written as Eq. (28), and it is not necessary to consider Eqs. (24), (25), and (26):

$$ROCOF^{sc}_n = \frac{f_0}{2H^{sc}}(\Delta FR^{sc}_n - \Delta GL^{sc} - D\Delta f^{sc}_n + \sum_s U^{sc}_{s,n} \times LSHS_s) \tag{28}$$

The amount of load shedding at each stage must be between zero and the total load of the system (TLS), according to Eq. (29):

$$\sum_s LSH_s \leq TLS \tag{29}$$

A successful load shedding scheme should be into under-frequency/time limitations of the generator specified by the manufacturer so that the generator would not be damaged if the frequency is dropped for a more extended period than a certain threshold. In Table 3, the limitations of the generators' under-frequency/time are shown.

Assuming the number of n_c critical frequency threshold f_c, corresponding to the maximum allowed time specified by the manufacturer Δt^{max}_c, a binary variable $W^{sc}_{c,n}$ is introduced under Eqs. (30) and (31):

$$\frac{f_c - (f_0 + \Delta f^{sc}_n)}{M_3} \leq W^{sc}_{c,n} \leq 1 + \frac{f_c - (f_0 + \Delta f^{sc}_n)}{M_3} \tag{30}$$

$$W^{sc}_{c,n} = \begin{cases} 0 & f_0 + \Delta f^{sc}_n > f_c \\ 1 & f_0 + \Delta f^{sc}_n < f_c \end{cases} \tag{31}$$

Here, the parameter M_3 is also a large positive number. The time spent of the system frequency below a certain frequency threshold $f_c$in the scenario *sc* at the step time *n* is written as Eq. (32):

$$\Delta t^{sc}_{c,n} = \Delta t^{sc}_{c,n-1} + W^{sc}_{c,n}\Delta t \tag{32}$$

The generator time/under-frequency limitations for setting the under-frequency relay must be met according to Eq. (33):

$$\Delta t^{sc}_{c,n} \leq \Delta t^{max}_c \tag{33}$$

Also, concerning Eqs. (34) and (35), the system frequency deviation of the steady-state, in the last time step Δf^{sc}_N, for example, should be into a permitted limitation $\pm$ 0.5 Hz:

$$-0.5 \leq \Delta f^{sc}_N \leq 0.5 \tag{34}$$

$$\Delta f^{sc}_N = \left(\frac{-\Delta GL^{sc} + \sum_s Z^{sc}_{s,N}}{D + \frac{1}{R^{sc}}}\right) \tag{35}$$

Here, $Z^{sc}_{s,N} = U^{sc}_{s,N} \times LSH_s$ is the load shedding amount in scenario *sc* and last time step N.

The constraint in Eq. (34) does not eliminate the frequency oscillations close to the steady-state and at the end of the simulation, so in order to eliminate these oscillations, the average frequency on the last time steps of nl, $\frac{1}{nl}\sum_{N-nl} \Delta f^{sc}_n$, close to the steady-state should be following Eq. (36) within the small range of $\hat{A} \pm 0.5Hz$:

$$-0.5 \leq \Delta f^{sc}_N - \frac{1}{nl}\sum_{N-nl} \Delta f^{sc}_n \leq 0.5 \tag{36}$$

In order to avoid the load shedding untimely, the frequency set-point f_s must be located within the permissible range of the under-frequency of the generator, in which this constraint is expressed in Eq. (37):

$$\min_c(f_c) \leq f_s \leq f_{max} \tag{37}$$

Besides, the condition in Eq. (38) must be considered to avoid having the same frequency set-points in the sequential stages of load shedding.

$$0.2Hz \leq f_s - f_{s+1} \tag{38}$$

2.2.4. Wind, solar, and load fluctuation modeling

The variations of the wind and solar generation and continuous load fluctuations affect the frequency of the system, and therefore these factors should be used to set the under-frequency relay. Hence, by Eq. (39) the terms of wind generation, ΔP^{sc}_w, solar generation, ΔP^{sc}_{pv} and load fluctuations, ΔP^{sc}_{lf}, are added to Eq. (8):

$$ROCOF^{sc}_n = \frac{f_0}{2H^{sc}}(\Delta FR^{sc}_n - \Delta GL^{sc} - D\Delta f^{sc}_n - \Delta P^{sc}_w - \Delta P^{sc}_{pv} - \Delta P^{sc}_{lf} + \sum_s U^{sc}_{s,n} \times LSH_s) \tag{39}$$

Table 3
Under-frequency/time limitations of a sample generator [25].

Allowed time (s)	Frequency (Hz)
Safe operation	59.5–60.5
30	59.5
15	58.5
1	57.5
0	56.5

2.2.5. Objective function

Three sets of design parameters for the setting of the under-frequency relay are considered as MILP decision variables: (1) Frequency set-points, f_s; (2) Time delay before the load shedding, Δt_s; and (3) The amount of load shedding at each stage LSH_s. Notice that, the UFLS problem has a large number of variables as well as constraints, it is difficult to achieve a possible solution and optimal value by using innovative and trial and error methods. The under-frequency relay setting protects the power system against all scenarios with different probability of occurrence. So, an appropriate objective function to minimize the load shedding value is considered as Eq. (40):

$$\min(F) = \min\left\{\sum_{sc}\left(\pi^{sc}\sum_{s} U^{sc}_{s,n} \times LSH_s\right)\right\} = \min\left\{\sum_{sc}\left(\pi^{sc}\sum_{s} Z^{sc}_{s,N}\right)\right\} \quad (40)$$

Here, the probability of each scenario is represented by π^{sc}, and if this probability is not known, it is estimated by a constant number $1/n_\pi$. Here, n_π is the number of scenarios that have a significant effect on the amount of load shedding.

Fig. 4 shows the proposed UFLS approach based on the MILP formulation. According to this figure, the proposed UFLS approach is implemented in two phases. The scenario generation process is addressed in the first phase given the various uncertainties. In the second phase, the scenarios resulted in the first phase are taken into account by the MILP formulation, and the three relay parameters are achieved. Finally, the proposed UFLS strategy is designed to obtain a suitable system frequency response.

3. Simulation results

To implement the proposed approach, two different types of simulation are performed on the IEEE 39-bus test system, which is described below:

- Simulation for validation of the proposed UFLS scheme
- Simulation in a scenario-based stochastic framework

All of the simulations in this paper have been implemented in 200 steps. In Fig. 5, the schematic of the IEEE 39-bus test system, with 10 generators and 19 loads, as well as with three wind farms and two solar farms, has been shown to design the proposed UFLS scheme. Hence, related system parameters to simulate the proposed scheme are presented in Tables 4 and 5. All values of these tables are expressed on the power base of 100MVA. Here, the effect of the uncertainties of the RES and load fluctuations on the proposed scheme should be investigated.

3.1. Simulation results for validation of the proposed UFLS scheme

In this section, eight contingencies pertaining to loss of generation have been considered for validation of the proposed method. In Table 6, the relevant information is presented for this purpose. Here, it is assumed that contingency intensity is gradually decreased from 0.5 to 0.1588 pu for contingency-1 to contingency-8, and the relay for each contingency is separately set, so that the under-frequency relay sheds the excessive load to prevent frequency collapse in one stage. Moreover, the variations in RES power and load fluctuations are not considered.

According to Table 7, given the decrease in generation deficiency (as shown in Fig. 6), the under-frequency relay performs load shedding at a higher set-point frequency. In fact, as generation deficiency decreases, so does frequency drop and ROCOF, and whenever the amount of ROCOF decreases, system frequency immediately returns to the safe range, between 59.5 and 60.5 Hz. Thus, if frequency is recovered without relay action, it will not be necessary to activate the under-frequency relay. Thus, as contingency intensity increases, frequency drops further, and does not return to the permissible range. Depending on contingency intensity, load shedding should occur at different frequencies.

According to Table 7, as contingency intensity decreases, the amount of load shedding is reduced from 0.407 pu in contingency-1 to 0 pu in contingency-8 at one stage. Since the frequency in contingency-8 is automatically restored, the under-frequency relay is not activated, and the amount of load shedding is zero. Time delay in all the contingencies is the constant value of 0.2 s. In Fig. 6, the system frequency waveform for a particular contingency is shown with and without a consideration of the action of the under-frequency relay. It is clear from the figure that if the relay does not shed the overload, the frequency severely will drop, and exceeds the allowable range.

Fig. 7 shows, according to the information in Table 6, the system frequency waveform resulting from the occurrence of the eight hypothetical contingencies. Based on this figure, the under-frequency relay has been well able to restore frequency within the acceptable range (60 ± 0.5 Hz) against all of the target contingencies. In Figs. 8 and 9, the variations in ROCOF and $|f_0 - f_{nadir}|$, respectively, have been shown for contingency-1 to contingency-8, where f_{nadir} is the minimum system frequency for each load shedding stage. According to both figures, as contingency intensity decreases, ROCOF and $|f_0 - f_{nadir}|$ are also reduced.

3.2. Simulation results in a scenario-based stochastic framework

In this section, three different scenarios are considered for the setting of the under-frequency relay for analysis of the proposed approach. In these scenarios, the uncertainties resulting from the generation deficiency of the main generators, variation in the wind and solar generation, and load fluctuations are considered. Hence, 1000 different scenarios are generated using the method based on the MCS and RWM for generation of the above three scenarios. Then, the three remaining

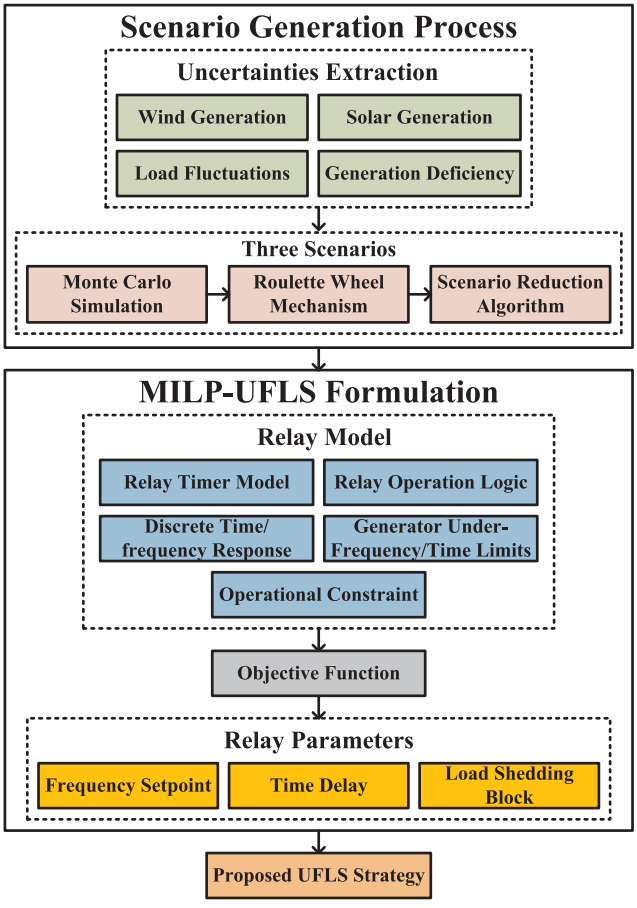

Fig. 4. Block diagram of the proposed UFLS scheme.

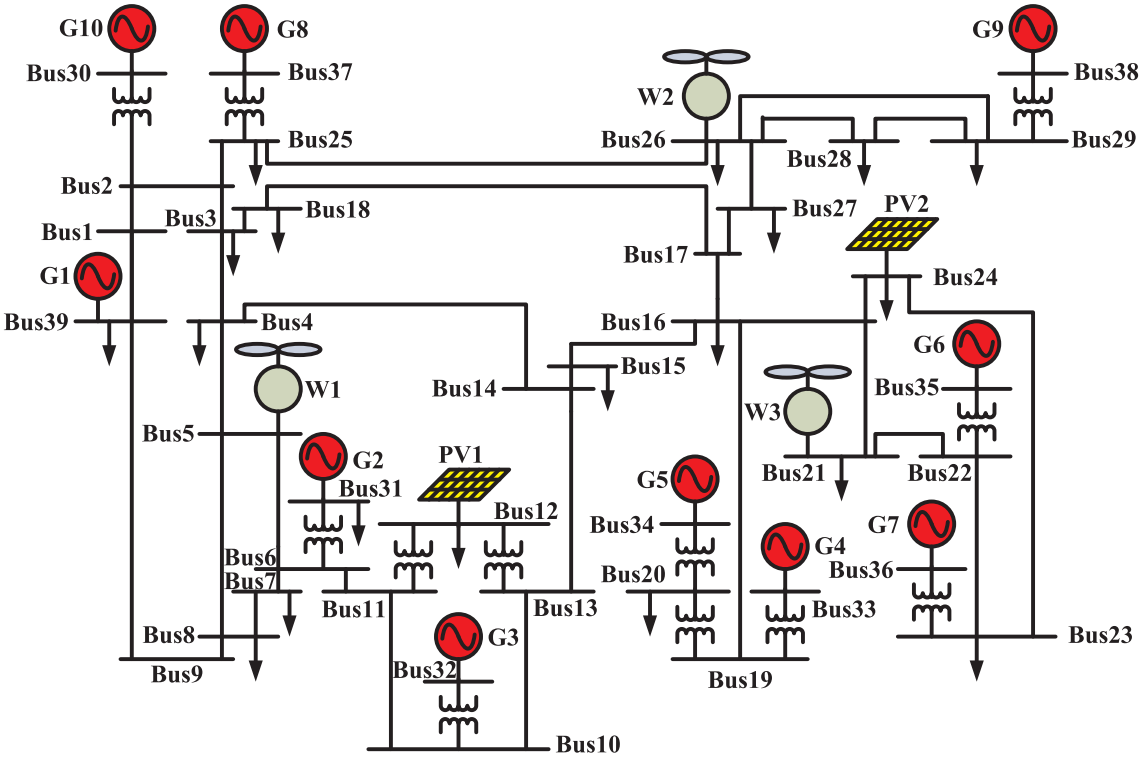

Fig. 5. Schematic diagram of the IEEE 39-bus system [26].

Table 4
Input parameters for the IEEE 39-bus system for simulation of the UFLS scheme [26].

Nominal frequency of the system, f_n (Hz)	60
The time constant of the equivalent inertia, H (s)	4
Load damping, D (pu)	2
governor equivalent droop, R (%)	5
Minimum frequency difference between consecutive stages of load shedding, Δf_{min} (Hz)	0.1

scenarios are selected as the most probable scenarios using the scenario reduction algorithm to optimize the parameters of the proposed under-frequency relay. In Table 8, the three scenarios concerning the proposed UFLS scheme are shown in the stochastic space to set the under-frequency relay. Table 9 shows the contingency information on Scenarios 1, 2, and 3 to implement the proposed UFLS scheme in the stochastic space. According to this table, Scenario 1 includes the mildest contingency, and Scenario 3 involves the most severe.

In Table 10, the simulation results in the stochastic space are presented for evaluation of the proposed scheme. In this table, two cases 1 and 2 are considered. In case 1, the generation deficiency of the main generators (merely contingency) is included, and there is no RES generation or load fluctuation in the test system. In this case, an amount of load of 0.433 pu has been shed in four stages. In case 2, wind and solar generation and incremental load fluctuation are considered as well as the contingency of the generation deficiency. The RES seeks to maintain the balance between generation and consumption. Hence, some overload is imposed on the system in different scenarios through reduction of the RES power and increase in the load fluctuations in the power

Table 6
Information used for validation of the proposed UFLS scheme.

Contingency No.	Generation deficiency (pu)	Equivalent inertia constant (s)	Equivalent drop of governor (%)	Number of lost generators
Contingency-1	0.5	2	6	2–3–4–6–8
Contingency-2	0.4432	2.4	5	1–2–3–5
Contingency-3	0.403	2.4	5	2–3–6–7
Contingency-4	0.3538	2.4	5	2–3–6–10
Contingency-5	0.3065	2.8	4.286	7–8–9
Contingency-6	0.2553	2.8	4.286	5–7–8
Contingency-7	0.1986	3.2	3.75	1–10
Contingency-8	0.1588	3.6	3.33	1

Table 7
Simulation results for validation of the proposed UFLS method.

Contingency No.	Set-point frequency f_s, (Hz)	Time delay Δt_s, (s)	The amount of the load shedding LSH_s, (pu)
Contingency-1	57.834	0.2	0.407
Contingency-2	58.182	0.2	0.333
Contingency-3	58.329	0.2	0.293
Contingency-4	58.508	0.2	0.244
Contingency-5	58.759	0.2	0.180
Contingency-6	58.946	0.2	0.129
Contingency-7	59.110	0.2	0.055
Contingency-8	–	–	–

Table 5
Nominal outputs of the system generators (pu) [26].

Gen1	Gen2	Gen3	Gen4	Gen5	Gen6	Gen7	Gen8	Gen9	Gen10
0.1588	0.1076	0.1032	0.1003	0.0806	0.1032	0.0890	0.0857	0.1318	0.0398

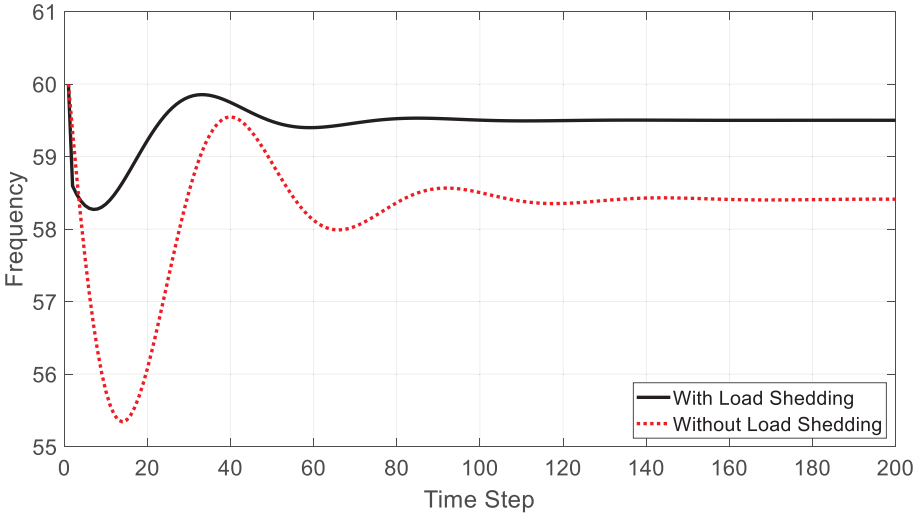

Fig. 6. Contingency of generation deficiency with and without under-frequency load shedding.

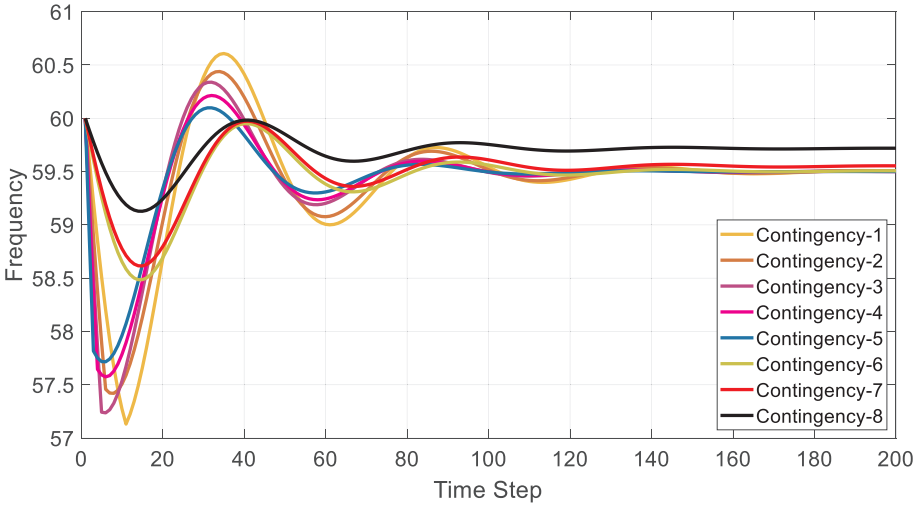

Fig. 7. Contingency of generation deficiency with under-frequency relay action for the eight contingencies.

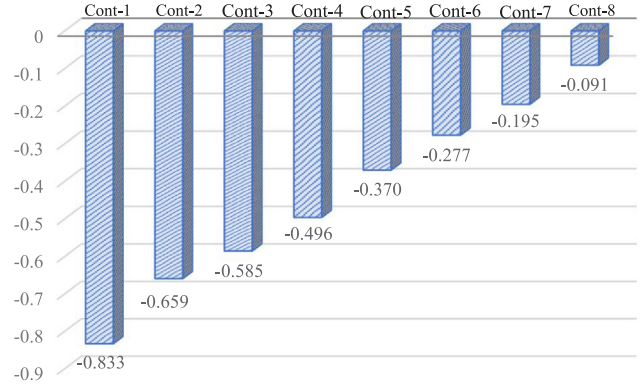

Fig. 8. Changes in the ROCOF value for contingency-1 to contingency-8.

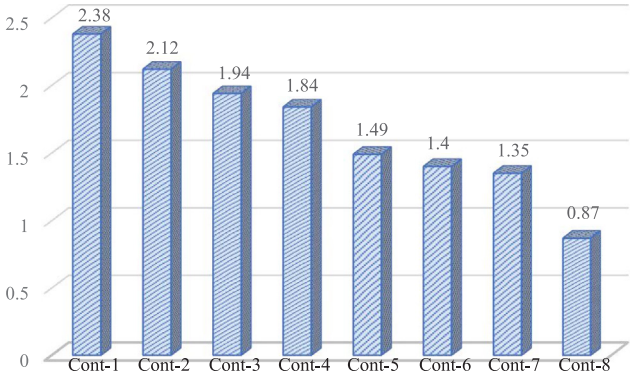

Fig. 9. Changes in the $|f_0 - f_{nadir}|$ value for contingency-1 to contingency-8.

system. In this case, the under-frequency relay successfully sheds 0.533 pu of the overload, and the proposed UFLS thus sustains the frequency within the safe range. The time delay in each of the four stages is 0.2 s for both cases. Moreover, the contingency intensity in case 1 is less than that in case 2, and the under-frequency relay sheds the overload at higher frequencies as a result.

Fig. 10 represents the frequency of the system in three Scenarios 1, 2, and 3 in both cases 1 and 2. According to the figure, the primary oscillation of frequency in case 1, which has a milder contingency intensity on the system, is lower, and frequency settles at points above 59.5 Hz in both cases. The generator under-frequency/time limitations have also been respected in both cases.

In Fig. 11, the proposed UFLS scheme is shown in four stages, which are plotted for cases 1 and 2 according to the results in Table 10. It is clear from a comparison of the two figures that different stages of load

Table 8
Presented scenarios for evaluation of the proposed UFLS in the stochastic space.

Scenario No.	Contingency resulting from generation deficiency*										System energy fluctuation (%)		
	G1	G2	G3	G4	G5	G6	G7	G8	G9	G10	Wind	Solar	Load
Scenario1	1	1	1	1	0	1	0	1	1	1	−7.5	−4	5
Scenario2	0	1	1	1	1	1	1	1	0	0	0	−8.5	25
Scenario3	1	0	0	0	1	0	1	0	1	1	−15	−11	25

* 1 where the generator is available and 0 otherwise.

Table 9
Contingency information for evaluation of the proposed UFLS in the stochastic space.

Scenario No.	Generation deficiency (pu)	Equivalent inertia constant (s)	Equivalent droop of the governor (%)	Number of lost generators
Scenario1	0.17	3.2	3.75	5–7
Scenario2	0.33	2.8	4.286	1–9–10
Scenario3	0.50	2	6	2–3–4–6–8

shedding are performed at lower frequencies in case 2 than in case 1 due to the higher intensity of contingency. Here, the gradient of each stage represents the ROCOF value in that stage. According to the figure, as the intensity of contingency in different scenarios of each case increases, so do the ROCOF and $|f_0 - f_{nadir}|$ values, as a result of which the value of f_{nadir} decreases. Therefore, f_{nadir} falls farther away from the reference frequency ($f_0 = 60$ Hz).

In the problem of optimizing the under-frequency relay settings, the term ENLS represents the expected load not served. Therefore, the ELNS index, used to assess the reliability and security of the system, can be written as in Eq. (41) [27,28].

$$ELNS = \sum_{sc} \pi^{sc} \sum_{s} LSH_s \quad (41)$$

The ELNS values for case 1 and case 2 in the stochastic space are 0.663 and 0.987, respectively. Therefore, the value of ELNS in case 2 is significantly higher than that in case 1, and the reliability and security of the system have decreased consequently. Although the ELNS value has increased, and the reliability and security of the system have been reduced, the proposed UFLS approach has been prevented system frequency collapse [29,30].

4. Discussion

The results of the proposed UFLS strategy are compared in Table 11 with those of three references [12,16], and [17]. In these works, as in the approach presented in this paper, mathematics-based strategies are used. In all of these studies, the purpose of UFLS is to minimize the amount of load shedding to enhance the reliability and security of the power system. Figs. 12–14 show the diagrams of the methods presented in [12,16], and [17].

In reference [12], 80 possible contingencies have been considered from 0.03 to 0.5 pu generation deficiency for protection of the system against a maximum of 50% generation loss. Then, five contingencies have been considered in the MILP formulation for the under-frequency relay setting using the umbrella contingency approach. These include the mildest contingency (0.15 pu generation deficiency) requiring load shedding, the most severe contingency (0.5 pu generation deficiency), and three contingencies in between (0.28, 0.33, and 0.4 pu generation deficiency). In this method, an amount of 0.44 pu of load has been shed.

In [16], the proposed deterministic UFLS scheme for the worst contingency of generation deficiency have been first optimized. Therefore, this is a very conservative approach. Here, a load block of 0.670 pu has been shed in four stages with time delays of 0.2 s. The set parameters have been optimized in the MILP formulation using the BONMIN solver. In the second part of this paper, the 3-PEM approach has been used to model the uncertainty of contingency. Then, the UFLS system parameters have been optimized at different stages given the uncertainty of generation deficiency. In this case, a load value of 0.454 pu has been shed, where the amount of load shedding is less than that in the previous case.

In [17], the probabilistic UFLS scheme has been implemented in two steps using the MILP formulation. In the first step, MCS is used to model the uncertainties resulting from generation deficiency, inertia constant, and load damping. A normal PDF is specified as a function of generation for these uncertainties. In the second step, using the mean value of the load to be shed (equal to 0.479 pu), four deterministic strategies have been planned, including increasing, decreasing, equal, and sandwich. This mean value has been considered as the maximum permissible load shedding. Thus, the parameters of under-frequency relay have been obtained optimally in this stage without maximum load shedding being exceeded. In this approach, a load of 0.480 pu has been shed in four stages for any strategy.

As shown in Table 11, the total load shedding in case 1 of the proposed UFLS approach is lower than those in the other references, which demonstrates the high efficiency of this approach. The use of MCS, RWM, and the scenario reduction algorithm process for specification of the optimal scenarios has increased the efficiency of the proposed UFLS method, and consequently reduces the amount of load shedding. In the references addressed, the effect of RES and load fluctuation has not been considered, as in case 1 in this paper, and mainly case 1, as an underlying case, has therefore been compared. After all,

Table 10
Simulation results in stochastic space to evaluate the UFLS proposed scheme.

Case No.	Set-point frequency f_s (Hz)				Time delay Δt_s (s)				Load shedding block LSH_s (pu)			
	St.1	St.2	St.3	St.4	St.1	St.2	St.3	St.4	St.1	St.2	St.3	St.4
Case1	59.022	58.734	58.544	58.293	0.2	0.2	0.2	0.2	0.103	0.195	0.074	0.061
									Sum = 0.433			
Case2	58.865	58.513	58.182	57.854	0.2	0.2	0.2	0.2	0.114	0.170	0.149	0.100
									Sum = 0.533			

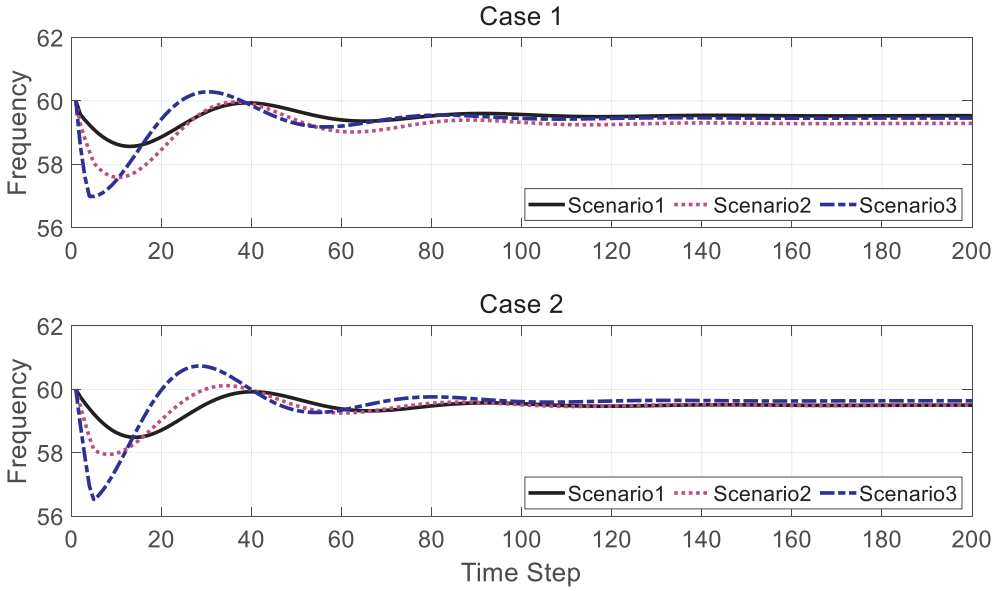

Fig. 10. System frequency waveform caused by Scenarios 1, 2 & 3 in cases 1 & 2.

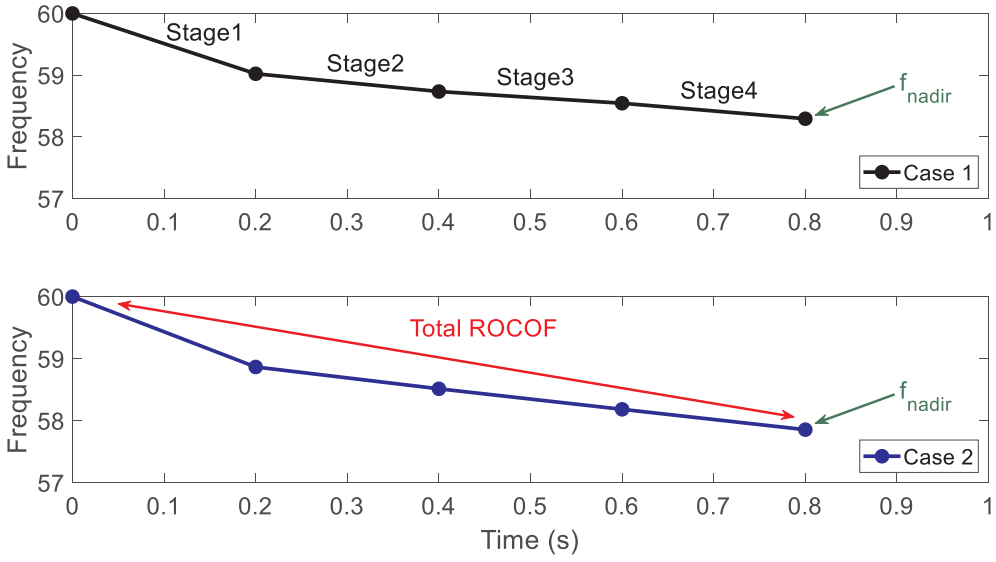

Fig. 11. Different stages of load shedding in cases 1 & 2.

Table 11
Comparison of the results of the proposed UFLS strategy with that of various references.

Load shedding method		Amount of load shedding
Proposed UFLS strategy	Case 1	0.433
	Case 2	0.533
Reference [12]		0.440
Reference [16]	Deterministic	0.670
	Probabilistic with 3-PEM Method	0.455
Reference [17]	Increasing	0.480
	Decreasing	
	Sandwich	
	Equality	

Table 11 also contains a comparison of case 2, involving the effects of RES and load fluctuation as well as contingency, both to the strategies adopted in the references and to case 1 in the present paper. As observed, case 2 exhibits an increase in load shedding, which, of course, results from the effect of RES and load fluctuation on system frequency. The results of case 2, however, are promising as long as it has successfully restored system frequency into the safe range. In all the strategies presented in this table, time delay is 0.2 s. All of these methods shed excessive loads at different frequency set-points in four stages.

5. Conclusion

In this paper, an innovative UFLS scheme based on MILP has been proposed. In the proposed approach, three different scenarios have been generated by a process involving MCS, RWM, and the scenario reduction algorithm given the uncertainties caused by the generation deficiency of the main generators, variations in RES power, and load fluctuations. Then, the amount of load shedding has been minimized, and the under-frequency relay parameters have been optimally set. The simulation results indicate the high performance of the proposed approach. Through the more precisely modeling of stochastic based uncertainties, the amount of load to be shed optimized more effectively.

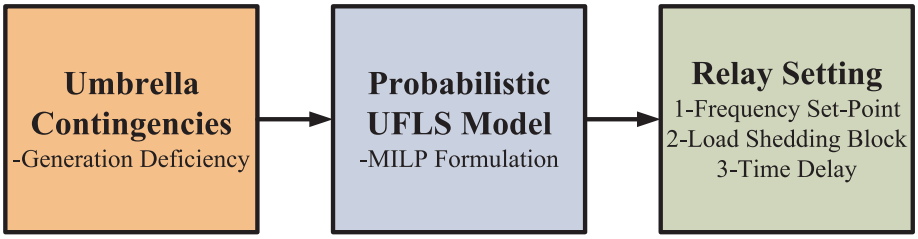

Fig. 12. Block diagram of the method presented in [12].

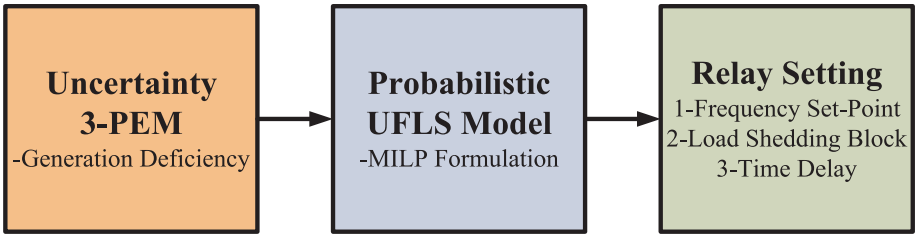

Fig. 13. Block diagram of the method presented in [16].

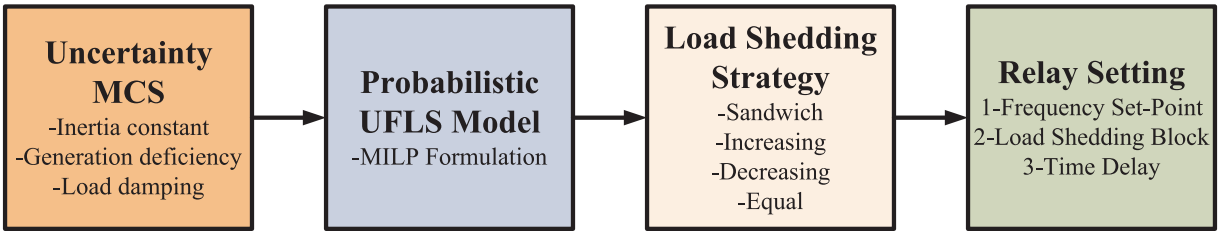

Fig. 14. Block diagram of the method presented in [17].

Due to the proposed linearized optimization framework, the derived solutions laid into the more trackable and near-global portfolio. Meanwhile, the conducted UFLS problem is comprehensive due to considering more extensively uncertainty resources. The key findings of the paper are summarized below.

- The frequency of the system has been protected against a variety of contingencies caused by the generation deficiency of the main generators with a minimum amount of load shedding.
- The frequency instability of the system, resulting from the uncertainties that are in turn to the RESs and load fluctuations, has been prevented from.
- Through reduction of load shedding, the security and reliability of the system have been increased.

Future works can consider use of demand response as a suitable means of facing the destructive effects of the various uncertainties in the power system.

References

[1] Billinton R, Allan RN. Reliability evaluation of power systems. New York: Plenum; 1996.
[2] Wu L, Shahidehpour M, Li T. Cost of reliability analysis based on stochastic unit commitment. IEEE Trans Power Syst 2008;23:1364–74.
[3] Michalewicz Z. Genetic algorithm + data structure = evaluation program. New York: Springer-Verlag; 1996.
[4] Amjadi N, Aghaei J, Shayanfar HA. Stochastic multiobjective market-clearing of joint energy and reserves auctions ensuring power system security. IEEE Trans Power Syst 2009;24:1841–54.
[5] Lai CS, Tao Y, Xu F, Ng WW, Jia Y, Yuan H, et al. A robust correlation analysis framework for imbalanced and dichotomous data with uncertainty. Inf Sci 2019;470:58–77.
[6] Alizadeh B, Jadid S. Reliability constrained coordination of generation and transmission expansion planning in power systems using mixed-integer programming. IET Gener Transm Distrib 2011;5:948–60.
[7] Motto AL, Galiana FD, Conejo AJ, Arroyo JM. Network-constrained multi-period auction for a pool-based electricity market. IEEE Trans Power Syst 2002;17:646–53.
[8] Yu H, Chung CY, Wong KP, Zhang JH. A chance-constrained transmission network expansion planning method with consideration of load and wind farm uncertainties. IEEE Trans Power Syst 2009;24:1567–76.
[9] Lan H, Wen S, Hong YY, Yu DC, Zhang L. Optimal sizing of hybrid PV/diesel/battery in ship power system. Appl Energy 2015;158:26–34.
[10] Nguyen TA, Crow ML, Elmore AC. Optimum sizing of a vanadium redox battery system foe microgrid systems. IEEE Trans Sustainable Energy 2015;6:729–37.
[11] Gu W, Liu W, Zhu J, Zhao B, Wu Z, Luo Z, et al. Adaptive decentralized under-frequency load shedding for islanded smart distribution networks. IEEE Trans Sustainable Energy 2014;5:886–95.
[12] Gomez C, Qadri SS, Galiana F. Under-frequency load shedding via integer programming. IEEE Trans Power Syst 2012;27:1387–94.
[13] Ketabi A, Fini MH. Adaptive under frequency load shedding using particle swarm optimization algorithm. J Appl Res Technol 2017;15:54–60.
[14] Jallad J, Mekhilef S, Mokhlis H, Laghari JA. Improved UFLS with consideration of power deficit during shedding process and flexible load selection. IET Renew Power Gener 2018;12:565–75.
[15] Zhenglong S, Guowei C, Yuwei W, Jiarong S. A method for the design of UFLS schemes of regional power system using improved frequency response model. Int Trans Electr Energy Syst 2017;2365:1–11.
[16] Darenaghi MG, Amraee A. Dynamic multistage under frequency load shedding considering uncertainty of generation loss. IET Generat Transmiss Distribut 2017;11:3202–9.
[17] Amraee T, Darenaghi MG, Soroudi A, Keane A. Probabilistic under frequency load shedding considering RoCoF relays of distributed generators. IEEE Trans Power Syst 2018;33:3587–98.
[18] Hong YY, Wei SF. Multiobjective underfrequency load shedding in an autonomous system using hierarchical genetic algorithms. IEEE Trans Power Delivery 2010;25:1355–62.
[19] Hsu CT, Kang MS, Chen CS. Design of adaptive load shedding by artificial neural networks. IEE Proc – Gener Transm Distribut 2005;152:415–21.
[20] Moazzami M, Khodabakhshian A, Hooshmand RA. A new optimal under-frequency load-shedding method using hybrid culture-particle swarm optimization–co-evolutionary algorithm and artificial neural networks. Electr Power Compon Syst 2015;43:69–82.
[21] Atighechi H, Hu P, Ebrahimi S, Lu J, Wang G, Wang L. An effective load shedding remedial action scheme considering wind farms generation. Int J Electr Power Energy Syst 2018;95:353–63.
[22] Rezaei N, Kalantar M. Stochastic frequency-security constrained energy and reserve management of an inverter interfaced islanded microgrid considering demand

response programs. Int J Electr Power Energy Syst 2015;69:273–86.
[23] Rezaei N, Kalantar M. Hierarchical energy and frequency security pricing in a smart microgrid: an equilibrium inspired epsilon constraint based multi-objective decision making approach. Energy Convers Manage 2015;98:533–43.
[24] Rezaei N, Kalantar M. Smart microgrid hierarchical frequency control ancillary service provision based on virtual inertia concept: an integrated demand response and droop controlled distributed generation framework. Energy Convers Manage 2015;92:287–301.
[25] Kundur P, Balu N, Lauby M. Power System Stability and Control. 7th ed. New York: McGraw-Hill Inc; 1994.
[26] Pai A. Energy function analysis for power system stability. Springer Science & Business Media; 2012.
[27] Halevi Y, Kottick D. Optimization of load shedding system. IEEE Trans Energy Convers 1993;8:207–13.
[28] Karimi M, Wall P, Mokhlis H, Terzija V. A new centralized adaptive under-frequency load shedding controller for microgrids based on a distribution state estimator. IEEE Trans Power Delivery 2016;10:370–80.
[29] Rafinia A, Moshtagh J. A new approach to fault location in three-phase underground distribution system using combination of wavelet analysis with ANN and FLS. Electr Pow Energy Syst 2014;55:261–74.
[30] Rezaei N, Kalantar M. Economic–environmental hierarchical frequency management of a droop-controlled islanded microgrid. Energy Convers Manage 2014;88:498–515.